J Mater Sci: Mater Med (2008) 19:1587–1593
DOI 10.1007/s10856-007-3301-5

Mathematical modelling of the evolution of protein distribution within single PLGA microspheres: prediction of local concentration profiles and release kinetics

Francesco Mollica · Marco Biondi · Sara Muzzi · Francesca Ungaro · Fabiana Quaglia · Maria Immacolata La Rotonda · Paolo Antonio Netti

Received: 4 July 2007 / Accepted: 2 October 2007 / Published online: 8 November 2007

Abstract Protein release from poly(D,L-lactide-co-glycolide) (PLGA) microspheres in an aqueous environment is governed by the diffusion of the protein through an autocatalytically degrading polymeric matrix. Many attempts have been made to model the release rate of proteins from biodegrading matrices, but the transport parameters involved in the process are not fully established at the microscale level. The aim of this work was to develop a new mathematical model taking into account the temporal evolution of the radial protein distribution during release, and to provide physical insight into the relation between local transport features and microsphere degradation. The model was validated by comparing its predictions with the experimentally determined protein concentration profiles in PLGA microspheres loaded with tetramethylrhodamine-labelled bovine serum albumin (BSA-Rhod) as a model protein. Morphological studies were carried out by scanning electron microscopy (SEM), while release kinetics and time-dependent BSA-Rhod concentration profiles within the microspheres were studied by a confocal laser scanning microscopy (CLSM)-assisted technique. The model, based on a modification of Fick's second law of diffusion, could closely fit the experimental protein radial distribution profiles in the microspheres as a function of time. It is also a useful tool to ab initio design protein release devices using degrading matrices.

F. Mollica · S. Muzzi
Department of Engineering, University of Ferrara, via Saragat 1, 44100 Ferrara, Italy

M. Biondi · F. Ungaro · F. Quaglia · M. I. La Rotonda · P. A. Netti (✉)
CRIB-Interdisciplinary Research Centre on Biomaterials, University of Naples Federico II, Naples, Italy
e-mail: nettipa@unina.it

1 Introduction

Scaffolds able to sequester and release bioactive proteins, such as growth factors (GFs), with controlled and predictable kinetics are promising in tissue engineering [1]. In fact, the application of drug delivery fundamentals, leading to controlled delivery of GFs into the scaffold, may enable to trigger, control and guide the regeneration of complex tissues [2, 3]. In their native environment, GFs, acting at very low concentrations (pico to nanomolar), tightly control cell proliferation, migration and orientation through finely tuned spatial and temporal concentration gradients [4–7]. Therefore, a promising strategy to make bio responsive scaffolds is to include GF-releasing micrometric depots within the scaffold structure: besides protecting the labile GFs against inactivation, the release pattern of GFs could be adjusted, so that tiny amounts and known gradients of the bioactive molecules can be obtained in a controlled way.

Among drug delivery devices, biodegradable poly(lactide-co-glycolide) (PLGA)-based microspheres acting as single point sources when included in a collagen scaffold have demonstrated their potential for GF-delivery in tissue equivalents [8–10]. PLGA microspheres can protect proteins against biological inactivation and can release them for long time frames, and at specific times (e.g. multiple factors can be delivered at different time intervals [11]). Furthermore, the controlled spatial localisation of these GF-releasing devices may enable to guide not only the extent, but also the pattern of tissue formation [3]. More importantly, we have previously shown that the release rate of protein-loaded PLGA microspheres can be programmed by varying the formulation of PLGA depots so that, depending on the transport properties of the protein within the matrix, its final release kinetics can be controlled [11].

In this work we aimed at the mathematical modelling and prediction of the protein release kinetics from a single PLGA microsphere. A mathematical model can be a useful tool to design PLGA microspheres with a priori known release kinetics, but to develop such a model the understanding of the transport phenomena taking place at the single microsphere level is fundamental. Multiple attempts have been made to model protein release from biodegradable microspheres, all of which elucidate the release phenomenon basing upon a combined diffusion/degradation mechanism. In literature, release kinetics have been modelled taking into account the evolving porosity [12, 13], the decreasing molecular weight of the polymer [14, 15], the release time related to auto acceleration effects [16], or the separate contributions to protein delivery provided by diffusion, degradation and erosion [17]. In spite of this remarkable work of modelling, none of these models describes the time-dependent radial drug concentration profiles within a single microsphere.

Protein release from biodegradable PLGA-based devices in aqueous media is a complex phenomenon involving protein diffusion and bulk matrix degradation due to the hydrolytic rupture of the ester bond in the polymer backbone. Hydrolysis is triggered by the rapid water intrusion into the microsphere, leading to a temporally and spatially evolving microporous structure of the device [18–21]. PLGA degradation, in turn, produces acidic compounds, which are trapped in the microsphere bulk until soluble oligomers are formed, and the consequent pH decrease accelerates PLGA degradation [21–23], thus establishing an autocatalytic mechanism.

In this study, a new mathematical model that takes into account the autocatalytic degradation of PLGA has been introduced, thus providing insight into the relation between local transport features and microsphere biodegradation. In order to check the predictions of the model, PLGA microspheres encapsulating tetramethylrhodamine-labelled bovine serum albumin (BSA-Rhod) were prepared, embedded in collagen as a tissue equivalent and incubated at 37 °C for release. Next, the time-dependent radial distributions of the protein within the microspheres were determined through a confocal laser scanning microscopy (CLSM)-assisted technique [11] and the results compared with the time-dependent protein concentration profiles obtained with the model. Also, images of microsphere cross sections were obtained by scanning electron microscopy (SEM).

2 Experimental

2.1 Materials

Poly(lactide-co-glycolide) (uncapped PLGA 50:50; M_w 41.9 kDa; i.v. 0.5 dl/g) was purchased from Boehringer Ingelheim (Germany). BSA-Rhod was obtained from Molecular Probes Europe BV (The Netherlands). Type I collagen (Vitrogen®; 3.0 mg/ml; pH 2) was obtained from Nutacon (The Netherlands). Also, poly(vinyl alcohol) (PVA, Mowiol® 40–88) and sodium hydroxide from Sigma–Aldrich (USA), and Tissue-Tek® embedding medium from Sakura Finetek (USA) were employed.

2.2 Microsphere preparation and characterisation

Protein-loaded microspheres were prepared at the theoretical loading of 0.25 mg of BSA-Rhod per 100 mg of microspheres by a multiple emulsion-solvent evaporation technique as described elsewhere [11]. Briefly, BSA-Rhod was dissolved in water and emulsified into a PLGA/methylene chloride solution (15% w/v); the emulsion was added to aqueous PVA (0.5% w/v), and a double emulsion was generated by a high-speed mixer (Diax 900, Heidolph, Germany). Microspheres were then hardened by evaporating the organic solvent at room temperature under stirring, washed three times in distilled water and lyophilised.

Mean diameters were determined by laser light scattering (Coulter LS 100Q, USA; λ_{ex} = 750 nm) on a dispersion of freeze-dried microspheres in 0.5% w/v aqueous PVA. Actual loading was determined by dissolving microspheres in 0.5 N NaOH under stirring and subsequently quantifying BSA-Rhod in solution by a LS 55 Luminescence spectrometer (Perkin–Elmer Instruments, USA) at λ_{ex} = 553 nm and λ_{em} = 577 nm. The BSA-Rhod diffusion coefficient in collagen (D_c) was measured by fluorescence correlation spectroscopy (FCS) in combination with CLSM, as described elsewhere [11]. In order to study the internal morphological variations of the degrading microspheres, the devices were suspended (0.1% w/v) in phosphate buffer saline solution (PBS, 120 mM NaCl, 2.7 mM KCl, 10 mM phosphate salts, pH 7.4), and the suspension was placed on an undulating rocker platform (Stovall LifeScience Inc., USA; 15 rpm). At scheduled time intervals, microspheres were washed three times with distilled water and lyophilised. For SEM analysis, the devices were dispersed in Tissue-Tek® embedding medium, fixed in Cryomold® devices (Sakura Finetek, USA) and cryosectioned (Accu-Cut® SRM™ 200 Rotary Microtome, Sakura Finetek, USA) at −24 °C (section thickness: 10 μm).

2.3 Protein radial distribution profiles

Ultra-dilute microsphere dispersions in non-gelled collagen (final concentration: 1.2 mg/ml; pH adjusted to 7.4) were loaded into hollow microslides (0.2 × 2.0 × 20 mm, 0.2 mm wall thickness) (VitroCom Inc., USA) and incubated at 37 °C for collagen fibrillogenesis (30 min) and BSA-Rhod

release. Protein depletion within the single microspheres was quantified by CLSM (Carl Zeiss, Germany) using an Argon laser (λ_{ex} = 543 nm; λ_{em} = 572 nm). The fluorescence-concentration relation was established by analysing standard solutions in capillaries at known concentrations (0.2–2.0 mg/ml) for their average fluorescence intensity. A linear correlation ($R^2 > 0.99$) was found. No photobleaching was detected, thus fluorescence decrease could be ascribed to protein release only. Radial concentration profiles of BSA-Rhod in the microspheres were determined by converting the fluorescence distribution obtained by CLSM in the equatorial planes of the microspheres to non-dimensional concentration. The final profiles were averaged on at least 30 microspheres.

3 Results and discussion

3.1 Microsphere properties

The microspheres were homogeneous in size (mean diameter: 22.0 ± 1.5 μm) and encapsulated BSA-Rhod with high efficiency (≥98.0%). It was previously demonstrated that the chemically-controlled protein release from PLGA microspheres occurred with the same kinetics in both collagen and saline solutions under gentle agitation [11]. This strongly suggests that in both liquid suspension and gel systems the same changes in microsphere morphology occur. SEM images of the microsphere cross-sections showed the progressive formation of large, randomly dispersed cavities within the devices, thus confirming the well-known autocatalytic mechanism dominating protein diffusion/release (Fig. 1).

Adopting spherical symmetry, lengths were non-dimensionalised using the microsphere average radius R_s = 11.0 μm as the length unit. Thus, letting ρ denote the non-dimensional radial coordinate in a spherical polar coordinate system, t denote time, and $c = c(\rho,t)$ protein concentration, the concentration profiles could be normalised with respect to the initial cumulative BSA-Rhod loading in the microsphere:

$$\Gamma(\rho,t) = \frac{c(\rho,t)}{4\pi \int_0^1 \rho^2 c(\rho,0)\, \mathrm{d}\rho} \quad (1)$$

Figure 2a shows some of the normalised concentration profiles as a function of ρ. The initial non-uniform

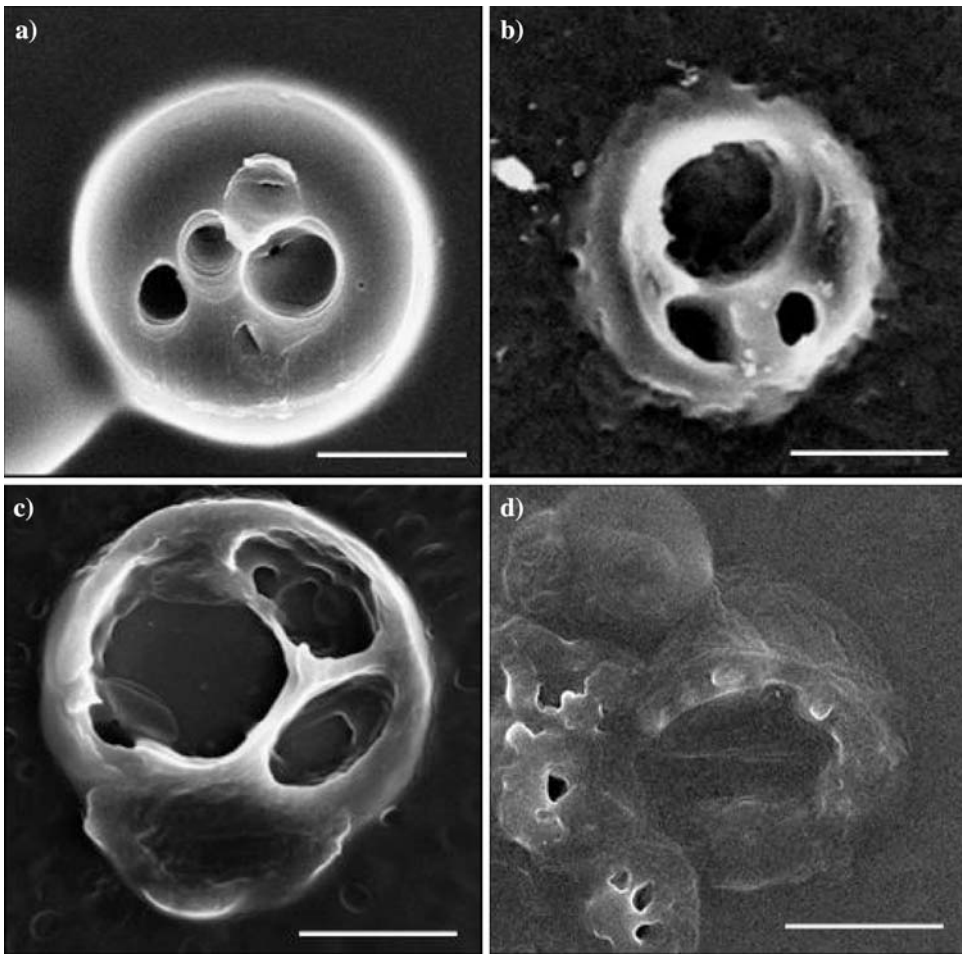

Fig. 1 SEM images of lyophilised, cryosectioned microspheres after 0 (**a**), 7 (**b**), 16 (**c**) and 23 days (**d**) of degradation. The bar is 10 μm

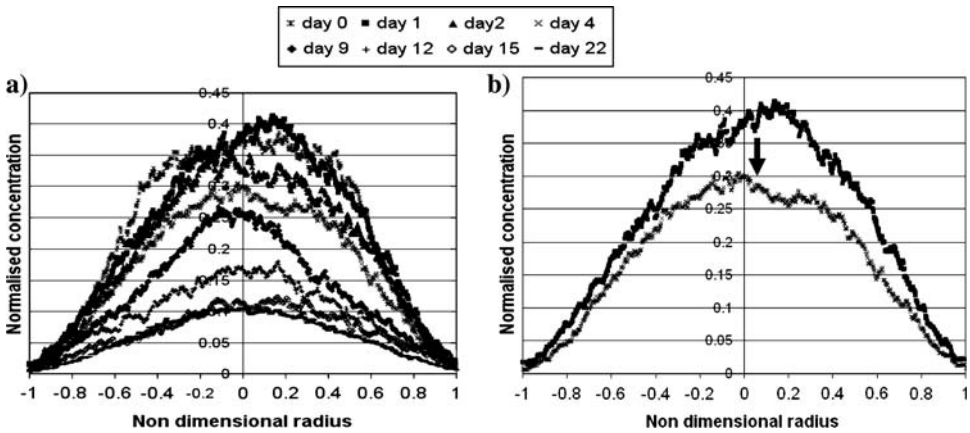

Fig. 2 (**a**) Experimental concentration profiles; (**b**) Protein depletion inside the microsphere occurs mainly in the microsphere centre, as indicated by the arrow

protein distribution retained its shape during the release phase.

3.2 Mathematical modelling

CLSM analysis of local protein concentration in equatorial cross-sections of the microspheres showed that the initial BSA-Rhod concentration decrease was located mainly in the central region of the microspheres (Fig. 2b), while being almost neglectable close to the microsphere boundary. This suggests that BSA-Rhod is able to diffuse out of the microspheres directly from the central region, seemingly without traversing the microspheres outer shell. A possible explanation for this puzzling phenomenon is pictured in Fig. 3: due to the preparation technique, BSA-Rhod is initially present only inside innate pseudospherical macropores isolated from the micropore network of the microsphere [12]; it is thus in an immobilised state (Fig. 3a). Therefore, protein mobilisation must occur via a

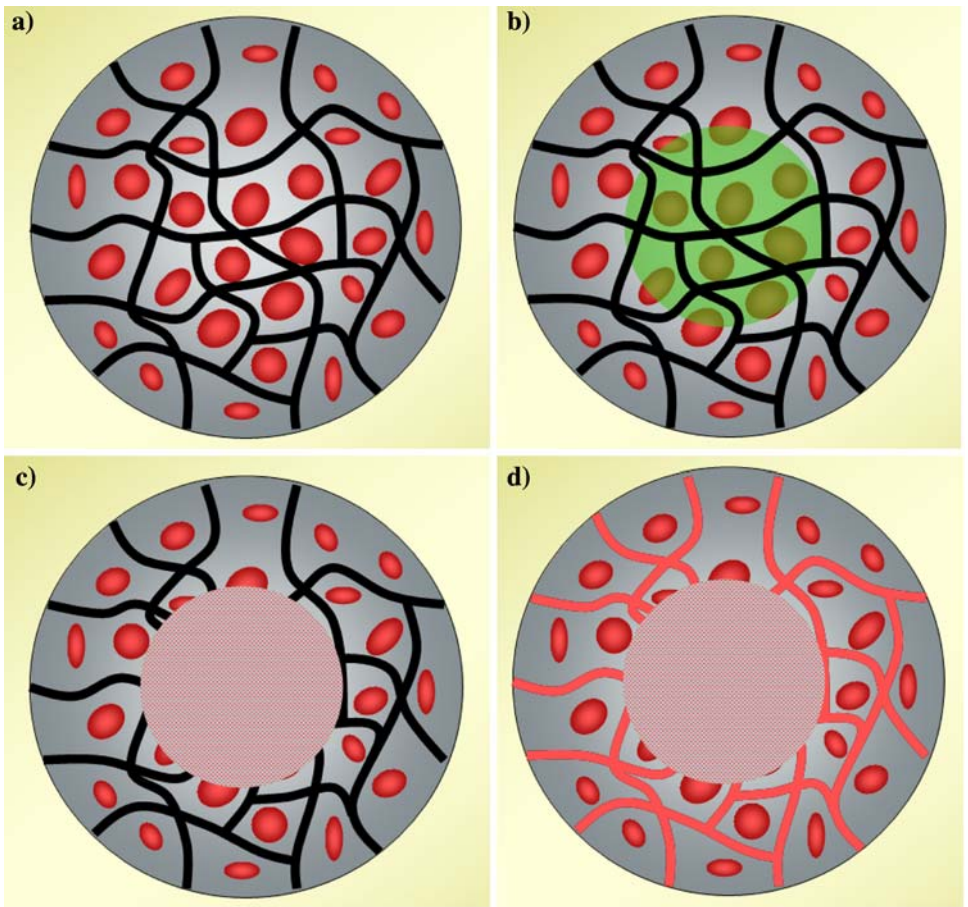

Fig. 3 The physical model: (**a**) microspheres contain the protein in pseudospherical macropores (*in red*) that are isolated from the micropore network (*in black*). (**b**) Microsphere degradation proceeds from the centre to the periphery following a degradation front (*in green*) that is assumed to keep spherical symmetry. (**c**) Inside the degradation front the isolated macropores become open and the protein is free to diffuse. (**d**) The protein (*in red*) exits the microsphere through the highly hydrated micropore network. In the outer shell protein concentration is basically unchanged

degradation-mediated macropore opening mechanism. Importantly, due to the autocatalytic PLGA degradation, macropore opening and hence triggering of protein transport are favoured in the microsphere centre, where pH is lower and the polymer is more extensively degraded; the peripheral macropores, on the other hand, mostly remain intact. As a result, protein mobilisation occurs following a degradation front that moves outwards from the centre (Fig. 3b). The mobilised protein can diffuse inside the degraded central region of the microsphere (Fig. 3c), while transport to the outside of the microsphere is allowed by the network of hydrated micropores (Fig. 3d) which, due to local degradation, are presumed to be large enough to allow rapid protein diffusion. With this mechanism, protein loss starts from the microsphere centre. On the other hand, protein concentration remains basically unchanged in the outer shell of the microsphere where protein is mainly located in the isolated, still unopened macropores. The presence of the degradation front can be inferred from the SEM scan of Fig. 1. In fact, large and progressively enlarging cavities are located in the microsphere centre, thus showing loss of matter preferentially from inner regions of the device and evoking the existence of the aforementioned degradation front.

In order to make the above physical model mathematically treatable, BSA-Rhod was divided into two populations: the immobile fraction Γ_{im} (contained in unopened macropores), and the mobile fraction Γ_{mb} (free to diffuse through the hydrated polymeric matrix). In this way, being $\Gamma(\rho, t)$ the total BSA-Rhod concentration:

$$\Gamma(\rho,t) = \Gamma_{im}(\rho,t) + \Gamma_{mb}(\rho,t). \tag{2}$$

Assuming spherical symmetry, mass conservation of both species is expressed by:

$$\begin{cases} \dfrac{\partial \Gamma_{mb}(\rho,t)}{\partial t} = \dfrac{1}{\rho^2}\dfrac{\partial}{\partial \rho}\left(\rho^2 D_{mb}(\rho,t)\dfrac{\partial \Gamma_{mb}(\rho,t)}{\partial \rho}\right) + \Phi(\rho,t) \\ \dfrac{\partial \Gamma_{im}(\rho,t)}{\partial t} = -\Phi(\rho,t) \end{cases} \tag{3}$$

where $D_{mb}(\rho,t)$ is the diffusion coefficient of the mobilised fraction and $\Phi(\rho,t)$ describes the conversion from the immobilised to the mobilised population. The same conversion term appears in both equations with opposite signs to superimpose conservation of the total BSA-Rhod concentration Γ. Both equations can be thought of as a modified Fick's second law: the first equation is Fick's second law with a source term, while the second is again Fick's second law with a zero diffusion coefficient (the immobilised species cannot diffuse) and a sink term.

To complete the model, specific forms have to be given for $\Phi(\rho,t)$ and for $D_{mb}(\rho,t)$. In particular, denoting with $R_f(t)$ the radius of the degradation front, it is assumed that

$$\Phi(\rho,t) = \begin{cases} k\Gamma_{im}(\rho,t) & \rho \le R_f(t),\ k \ge 0 \\ 0 & \rho > R_f(t) \end{cases} \tag{4}$$

i.e. conversion occurs only from immobilised to mobilised species and only inside the degradation front ($\rho \le R_f(t)$), following a first order kinetics with the rate constant k, and

$$D_{mb}(\rho,t) = \begin{cases} D_s & \rho \le R_f(t), \\ D_c & \rho > R_f(t), \end{cases} \tag{5}$$

i.e. the diffusion coefficient is piecewise constant across the degradation front. Its value outside the degradation front D_c is assumed to be equal to the BSA-Rhod diffusion coefficient in collagen, i.e. 4.16×10^{-7} cm^2/s [11]. This hypothesis is justified by the high hydration of the microchannels in which protein diffusion occurs [12]. It is further assumed that $D_s < D_c$, to describe the quicker diffusion of the mobilised species through the micropore network outside the degradation front. This assumption relies on the observation that in the central region a complex system formed by polymer and degradation products exists, which is reasonably more viscous than the highly hydrated environment of the micropore network. Concerning the degradation front, it is assumed that its position be given by a known function of time:

$$R_f(t) = h\sqrt{t}, \tag{6}$$

where h is an adjustable parameter. Concentration profiles as a function of time can be obtained by solving Eq. (3) subject to the appropriate initial and boundary conditions, respectively:

$$\begin{cases} \Gamma_{im}(\rho, 0) = \Gamma(\rho, 0) = \Gamma_0(\rho), \\ \Gamma_{mb}(\rho, 0) = 0, \end{cases} \tag{7}$$

$$\left.\frac{\partial \Gamma_{mb}}{\partial \rho}\right|_{\rho=0} = \left.\frac{\partial \Gamma_{mb}}{\partial \rho}\right|_{\rho\to\infty} = 0, \tag{8}$$

where $\Gamma_0(\rho)$ is the initial protein distribution. The solution was obtained numerically using the finite element method (FEM) implemented in MATLAB® 5.3 with a Crank–Nicholson time marching scheme [24]. The results of the FEM simulations were compared with the experimental data in Fig. 4a. The values of the four model parameters used in the simulations are listed in Table 1, while the correlation coefficients for each of the experimental curves are listed in Table 2. The model predictions are very accurate for shorter times, whereas for longer times (>15 days) the model underestimates the experimental values. This may be explained by considering that, after

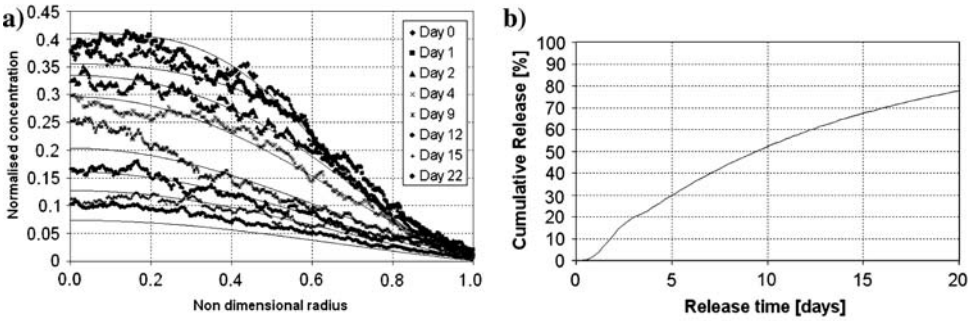

Fig. 4 (**a**) Comparison between model predictions (*straight lines*) and experimental BSA-Rhod profiles in PLGA microsphere radius after 0, 1, 2, 4, 9, 12, 15 and 22 days of release. (**b**) Cumulative release as a function of time predicted by the model. The lag time phenomenon is present within the first· day of release

Table 1 The values of the parameters used in the simulation

k (s^{-1})	h ($cm/s^{1/2}$)	D_s (cm^2/s)	D_c (cm^2/s)
1.95	6.05×10^{-4}	9.68×10^{-9}	4.16×10^{-7}

Table 2 R^2 values for the curve fitting of the model with the experimental data

Day 0	Day 1	Day 2	Day 4	Day 9	Day 12	Day 15	Day 22
0.965	0.956	0.982	0.986	0.930	0.967	0.917	0.681

several days of release, structural variations occur in the microsphere due to extensive degradation. At the same time, micropore closing is known to occur during release [25] and this is not taken into account by the model. The cumulative release profile, as predicted by the model, is pictured in Fig. 4b: release occurs after a time lag of about 1 day, in agreement with the results presented in [11].

4 Conclusions

Taken all together, the results confirm the well-known autocatalytic kinetics of PLGA degradation leading to material loss from internal sections of the devices. The proposed model provides some interesting clues to understand the complex interplay between protein transport and degradation phenomena controlling protein release from a single PLGA microsphere.

In tissue engineering applications, an accurate control over the concentration of proteins such as signalling, growth or morphogenetic factors, and their gradients has to be gained. This may be achieved by conveniently positioning protein-releasing PLGA microspheres within the scaffold. However, a continuous delivery of the released molecule, following a priori known release kinetics in the scaffold, is necessary to reach this aim. The present model, in establishing proper relationships between global and local properties, employs four parameters that characterise protein release. These parameters can be varied through an adequate microsphere formulation. The model can therefore be used to design microspheres with predetermined release profiles, so that protein gradients inside the scaffold can be sustained and customised. To this aim, the authors are currently working on an experimental protocol to quantify the model parameters with independent measurements in order to make the model completely predictive. This work is underway and will be published in a forthcoming article.

References

1. M. C. PETERS, B. C. ISENBERG, J. A. ROWLEY, D. J. MOONEY, *J. Biomater. Sci. Polym. Ed.* **9** (1998) 1267
2. T. A. HOLLAND, A. G. MIKOS, *Adv. Biochem. Eng. Biotechnol.* **102** (2006) 161
3. F. UNGARO, M. BIONDI, L. INDOLFI, G. DE ROSA M. I. LA ROTONDA, F. QUAGLIA, P.A. NETTI (2005) Bioactivated Polymer Scaffolds for Tissue Engineering. In Topics in Tissue engineering Vol. II, edited by N. ASHAMMAKHI, R. L. RISE and W. SUN
4. D. F. LAZAROUS, M. SHOU, M. SCHEINOWITZ, E. HODGE, V. THIRUMURTI, A. N. KITSIOU, *Circulation* **94** (1996) 1074
5. N. FERRARA, H. P. GERBER, J. LECOUTER, *Nat. Med.* **9** (2003) 669
6. C. L. HELM, M. E. FLEURY, A. H. ZISCH, F. BOSCHETTI, M. A. SWARTZ, *Proc. Natl. Acad. Sci. USA* **102** (2005) 15779
7. H. GERHARDT, M. GOLDING, M. FRUTTIGER, C. RUHRBERG, A. LUNDKVIST, A. ABRAMSON, *J. Cell. Biol.* **161** (2003) 1163
8. J. ELISSEEFF, W. MCINTOSH, K. ANSETH, S. RILEY, P. RAGAN, R. LANGER, *J. Biomed. Mater. Res.* **51** (2000) 164
9. T. P. RICHARDSON, M. C. PETERS, A. B. ENNETT, D. J. MOONEY, *Nat. Biotechnol.* **19** (2001) 1029
10. A. PERETS, Y. BARUCH, F. WEISBUCH, G. SHOSHANY, G. NEUFELD, S. COHEN, *J. Biomed. Mater. Res.* **65A** (2003) 489
11. F. UNGARO, M. BIONDI, I. D'ANGELO, L. INDOLFI, F. QUAGLIA, P. A. NETTI, M. I. LA ROTONDA, *J. Control. Release* **113** (2006) 128
12. R.P. BATYCKY, J. HANES, R. LANGER, D. A. EDWARDS, *J. Pharm. Sci.* **86** (1997) 1464
13. V. LEMAIRE, J. BELAIR, P. HILDGEN, *Int. J. Pharm.* **258** (2003) 95
14. N. FAISANT, J. SIEPMANN, J. P. BENOIT, *Eur. J. Pharm. Sci.* **15** (2002) 355

15. N. FAISANT, J. SIEPMANN, J. RICHARD, J. P. BENOIT, *Eur. J. Pharmaceut. Biopharmaceut.* **56** (2003) 271
16. J. HE, C. ZHONG, J. MI, *Drug Deliv.* **12** (2005) 251
17. M. ZHANG, Z. YANG, L. L. CHOW, C. H. WANG, *J. Pharm. Sci.* **92** (2003) 2040
18. G. CROTTS, T. G. PARK, *J. Microencapsul.* **15** (1998) 699
19. H. OKADA, H. TOGUCHI, *Crit. Rev. Ther. Drug Carrier Syst.* **12** (1995) 1
20. T.G. PARK, *Biomaterials* **16** (1995) 1123
21. I. GRIZZI, H. GARREAU, S. LI, M. VERT, *Biomaterials* **16** (1995) 305
22. F. VON BURKERSRODA, L. SCHEDL, A. GÖPFERICH, *Biomaterials* **23** (2002) 4221
23. J. SIEPMANN, K. ELKHARRAZ, F. SIEPMANN, D. KLOSE, *Biomacromolecules* **6** (2005) 2312
24. J. N. REDDY, in "Introduction to the Finite Element Method" (McGraw Hill, 1993) 228
25. J. KANG, S. P. SCHWENDEMAN, *Mol. Pharm.* **4** (2007) 104